Advances in Engineering Research : Possibilities and Challenges
ISSN Print: 3079-5192
ISSN Online: 3079-5206
https://doi.org/10.63313/AERpc.9073

Research on the Influence of Magnetron Sputtering parameters on the Structure and Properties of ITO Thin Films

Dongfeng Ma[1]. PengCheng Zhang[2] and Dunzhu GeSang[1,*]
[1]Science and Technology on Vacuum Technology and Physics Laboratory, Lanzhou Institute of Physics, Lanzhou, China
[2]School of Mechanical and Electrical Engineering, Lanzhou University of Technology, Lanzhou, China
Email: 1171303254@qq.com

How to cite this paper: Ma, D. F., Zhang, P. C., & GeSang, D. Z. (2026). Research on the Influence of Magnetron Sputtering parameters on the Structure and Properties of ITO Thin Films. Advances in Engineering Research: Possibilities and Challenges, 3(2), 60–74. ISSN Print: 3079-5192; ISSN Online: 3079-5206.
https://doi.org/10.63313/AERpc.9073
Published: 2026-01-31

Abstract

This study systematically investigates the influence of key magnetron sputtering parameters—working pressure, sputtering power, and nitrogen doping—on the growth, microstructure, and functional properties of indium tin oxide (ITO) thin films. Through a designed experimental matrix, the deposition kinetics, crystallographic structure, chemical bonding states, and electrical resistivity were characterized to establish clear process-structure-property relationships. The results reveal that increasing the working pressure enhances oxygen vacancy concentration, which dominates the reduction in electrical resistivity despite a degradation in crystallinity. Higher sputtering power improves film crystallinity and dopant activation, synergistically optimizing carrier mobility and concentration. Nitrogen incorporation introduces complex doping effects, initially passivating oxygen vacancies to lower resistivity at low partial pressure but forming carrier-trapping nitride phases at higher levels, leading to increased resistivity and amorphization. This work provides a mechanistic understanding of parameter-controlled defect engineering and microstructure evolution in ITO films, offering practical guidance for tailoring their optoelectronic performance for advanced transparent electrode applications.

Keywords

ITO thin films; Magnetron sputtering; Structure; Properties

1. Introduction

Indium tin oxide (ITO) thin films, as representative transparent conductive oxide materials, have become indispensable functional components in modern optoelectronic devices due to their exceptional properties, including a wide bandgap (~3.5–4.3 eV), low resistivity (10^{-4}–10^{-3} Ω·cm), high visible-light transmittance (>85%), ultraviolet absorption, and infrared reflectivity [1]. These characteristics have enabled their widespread applications in liquid crystal displays, organic

light-emitting diodes, solar cells, thin films sensors, smart windows, and energy-efficient architectural glass [2-7]. Among various deposition techniques, magnetron sputtering stands out for its scalability, uniformity, and precise control over film composition, making it the preferred method for large-scale ITO production. However, the structural and optoelectronic properties of sputtered ITO films are highly sensitive to the deposition parameters employed during the process. Key parameters such as the applied sputtering power, the working gas pressure, and the partial pressure of reactive gases like nitrogen (N_2) exert profound influences. These parameters govern critical aspects of the deposition environment, including plasma energy density, collision frequency amongst species, and the resultant adatom mobility and energy upon arriving at the substrate. Consequently, they directly dictate the film's growth kinetics, microstructure (e.g., crystallinity, grain size, texture, density), stoichiometry, and defect chemistry (particularly oxygen vacancy concentration and tin doping efficiency). Variations in these structural and compositional attributes inevitably translate into significant changes in the functional properties of the films, such as electrical resistivity, optical transmittance, and mechanical stability.

Despite extensive research on ITO deposition [8-13], the intricate “synergistic” effects of these sputtering parameters, particularly when incorporating reactive gases such as nitrogen for specific property enhancements, remain inadequately understood. Nitrogen doping has emerged as a promising strategy to improve the thermal stability of ITO films, potentially mitigating performance degradation at elevated temperatures encountered in some applications [14,15]. The introduction of nitrogen can alter bonding configurations (e.g., forming In-N bonds), modify the defect landscape (affecting oxygen vacancy formation and migration), and influence the crystallographic orientation [16,17]. However, the precise mechanisms by which nitrogen partial pressure interacts with other fundamental parameters like power and total pressure to co-determine film characteristics are not fully elucidated. Previous studies often focus on the isolated effect of a single parameter, leaving a gap in understanding the complex interplay between power, pressure, and reactive gas environment. This lack of comprehensive knowledge hinders the precise optimization of the sputtering process for achieving tailored film properties, especially for advanced variants like nitrogen-doped ITO which demands a delicate balance between conductivity, transparency, and enhanced stability

Therefore, this study aims to systematically investigate the influence of critical sputtering parameters – specifically sputtering power, working pressure, and nitrogen partial pressure – on the structural evolution and functional performance of ITO thin films. We focus on understanding how these parameters, both individually and in combination, affect key outcomes including the deposition rate, electrical resistivity, crystallographic structure, and chemical composition/bonding states. By establishing clear correlations between the deposition conditions and the

resultant film properties, this work seeks to provide deeper insights into the growth mechanisms and defect formation processes in sputtered ITO.

2. Experimental

2.1. Preparation of ITO thin films

ITO thin films were deposited on thermally oxidized silicon wafers under different sputtering parameters using DC magnetron sputtering. To achieve precise characterization of thin film microstructures, single-crystal silicon (100) substrates with 200 nm thermally-grown SiO_2 film were employed as substrates. A 100mm-diameter ceramic target composed of In2O3/SnO2 (90 wt%/10 wt%) with 99.99% purity was used for thin films depositions. All ITO thin films were deposited at room temperature. An orthogonal experimental design was employed to investigate the effects of key deposition parameters. Firstly, ITO thin films were deposited under pure Ar atmospheres with working pressures set at 0.4 Pa, 0.6 Pa, and 0.8 Pa, while maintaining a constant DC sputtering power of 100 W, a target-to-substrate distance of 7 mm, and a substrate rotation speed of 10 rpm. Secondly, with the working pressure fixed at 0.6 Pa, depositions were conducted at sputtering powers of 50 W and 150 W, keeping the same target-to-substrate distance and substrate rotation rate. Furthermore, to examine the influence of nitrogen doping on the composition and properties of the films, ITO(N) films were deposited in an Ar+N_2 mixed atmosphere. These depositions were performed at a fixed total pressure of 0.4 Pa and a constant sputtering power of 100 W, with Ar/N_2 flow ratios set at 10:1 and 5:1, respectively.

Table 1. Sputtering parameters of ITO thin films

	Power (W)	Atmosphere	Pressure (Pa)
A4	100	Ar	0.4
A6	100	Ar	0.6
A8	100	Ar	0.8
P05	50	Ar	0.6
P15	150	Ar	0.6
N1	100	Ar:N2(10:1)	0.4
N2	100	Ar:N2(5:1)	0.4

2.2. Characterization and Testing

The crystallographic structures of the as-deposited and annealed ITO thin films were analyzed by X-ray diffraction (XRD, Smart Lab 3KW) with Cu-Kα1 radiation source (λ=1.5418Å). The composition and chemical state of the elements in the ITO thin films were determined by X-ray photoelectron spectroscopy (XPS, PHI 5000

Vesaprobe III, Japen) with a 1486.8 eV monochromatic Al K X-ray source. The binding energies of the spectra were calibrated with C1s at 284.6 eV. Peaking fitting was performed by MultiPak software and a linear background assumption. The surface morphology of the thin films was characterized by a field-emission scanning electron microscope (FE-SEM, Zeiss Gemini sigma 500).

The sheet resistance (R_s) of the ITO thin films was measured using a four-point probe resistivity measurement system. To eliminate the influence of film thickness variations on the sheet resistance, the electrical resistivity (ρ) of the films was calculated from the measured sheet resistance and the film thickness (t) according to the following formula:

$$\rho = R_S \times t \ (\Omega \cdot cm) \quad (1)$$

where R_s is the sheet resistance (Ω/□) and t is the film thickness (cm).

3. Results

3.1. Effect of Sputtering Pressure

An analysis of the deposition rates of ITO thin films under different working pressures revealed that within the range of 0.4–0.8 Pa, the deposition rate remained approximately 39 nm/min (**Table 2**). This indicates that the working pressure had no significant influence on the deposition rate. During sputtering, the effect of pressure on the deposition rate is governed by two competing mechanisms: on one hand, increasing the pressure raises the density of argon ions, thereby enhancing the number of ITO atoms sputtered from the target; on the other hand, a higher pressure increases the probability of collisions between ITO particles and argon atoms/ions in the chamber, which tends to reduce the deposition rate. As a result, the deposition rate exhibited a slight initial increase followed by a decrease under the combined influence of these two factors.

Table 2. Effect of Magnetron Sputtering Pressure on the Deposition Rate and Electrical Resistivity of ITO Thin Films

	Deposition rate nm/min	Sheet resistance Ω/□	Resistivity 10^{-4}Ωcm
A4	39.9	23.5	11.26
A6	40.5	30.6	9.93
A8	38.3	37.4	5.73

Resistivity measurements of the ITO films showed that as the pressure increased, the resistivity gradually decreased from 11.26×10^{-4} Ω·cm to 5.73×10^{-4} Ω·cm. This suggests that higher sputtering pressures improve the electrical conductivity of the films. This phenomenon may be related to the oxygen content in the ITO films deposited under different pressures. With increasing sputtering pressure, the collision probability between sputtered particles and the chamber gas increases. Low-energy oxygen ions are more likely to collide with argon atoms and thus are less likely to reach the substrate surface, leading to a higher concentration of oxygen vacancies in the ITO films and consequently enhanced conductivity.

Figure 1 presents surface and cross-sectional SEM images of the ITO films deposited

at different pressures, showing a dense as-sputtered structure. **Figure 2** displays the XRD patterns of the as-sputtered ITO films. To enhance the visibility of the diffraction peaks, the count rates were processed using a logarithmic function. With increasing pressure, the SEM surface morphology showed a clear reduction in particle size and agglomeration. In the XRD patterns, the intensities of the In_2O_3 diffraction peaks corresponding to the (222), (400), (440), and (622) planes gradually decreased, indicating a reduction in both surface roughness and crystallinity. Additionally, a satellite peak appeared near $2\theta \approx 32°$ in the XRD patterns and became more pronounced with increasing pressure.

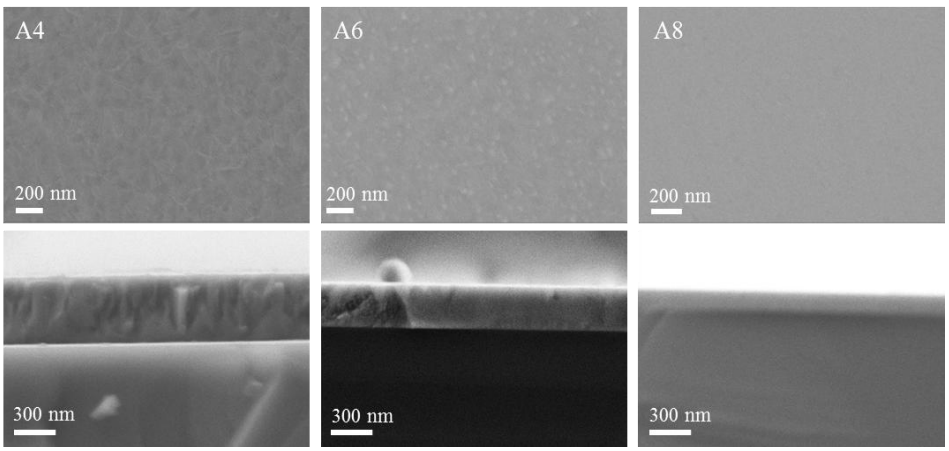

Figure 1 Surface and Cross-Sectional SEM Morphologies of ITO Thin Films Deposited at Different Pressures

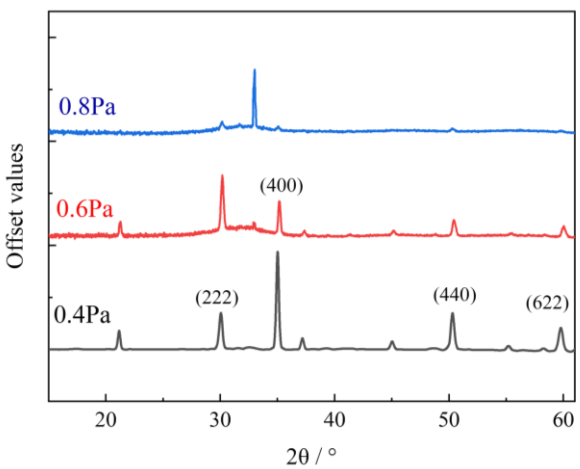

Figure 2. XRD Patterns of As-deposited ITO Thin Films

3.2. Effect of Sputtering Power

ITO thin films were deposited at DC sputtering powers of 50 W, 100 W, and 150 W, respectively, while keeping all other parameters constant. **Table 3** summarizes the corresponding deposition rates and electrical resistivities of the ITO films prepared

under different magnetron sputtering powers. As the sputtering power increased, the deposition rate rose significantly, while the resistivity gradually decreased. The enhancement in deposition rate with higher power is self-evident and thus not discussed in detail here. The improvement in electrical conductivity, however, requires further comprehensive analysis combining additional characterization techniques.

Table 3. Effect of Magnetron Sputtering Power on the Deposition Rate and Electrical Resistivity of ITO Thin Films

	Deposition rate nm/min	Sheet resistance Ω/□	Resistivity 10-4Ωcm
P05	20.5	50.0	12.3
P10(A6)	40.5	30.6	9.93
P15	56.6	27.5	9.33

Figure 3 presents secondary electron images for ITO films deposited at different sputtering powers. It can be observed that films sputtered at high power (150 W) exhibit a columnar grain structure with grain sizes ranging from 100 to 200 nm. Reducing the sputtering power leads to a gradual decrease in grain (agglomeration) size. This indicates that increasing the sputtering power raises the energy of particles arriving at the substrate surface, which promotes nucleation and growth of grains within the film.

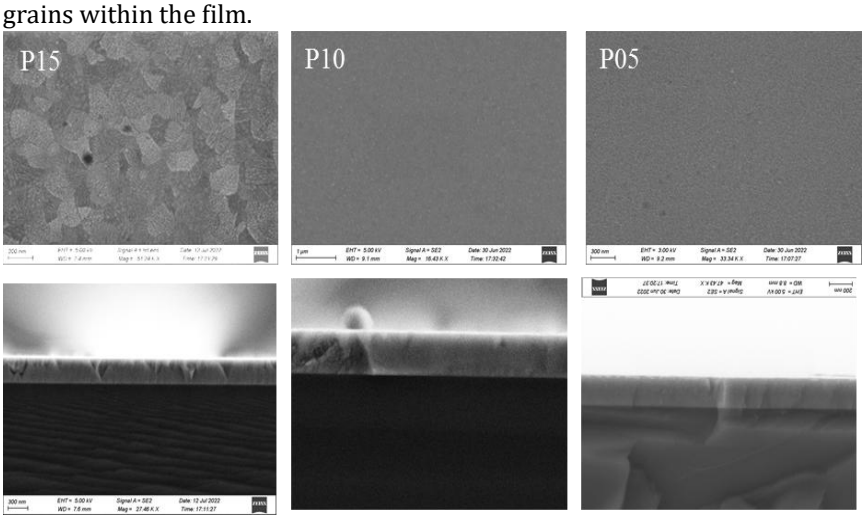

Figure 3. Surface and Cross-Sectional SEM Morphologies of ITO Thin Films Deposited at Different power

XRD analysis revealed that no characteristic In_2O_3 peaks were detected in the film deposited at 50 W, as shown in Figure 4, suggesting that the low energy of sputtered particles at this power results in a predominantly amorphous structure. When the power was increased to 100 W and 150 W, multiple In_2O_3 diffraction peaks, such as (211), (222), (400), and (440), became clearly visible, confirming good crystallinity of the films without a pronounced preferential growth orientation.

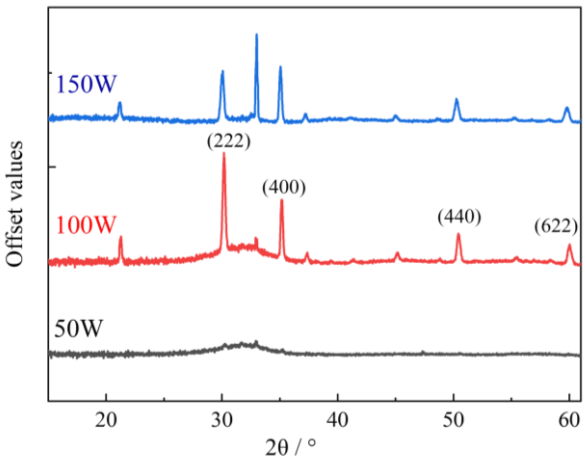

Figure 4. XRD Patterns of As-deposited ITO Thin Films sputtered under different power

3.3. Effect of Nitrogen Doping

Table 4 presents the deposition rates and electrical resistivity data of ITO films deposited under different nitrogen partial pressures. When the N_2/Ar flow ratio increased from 0 to 1:10, a slight decrease in deposition rate was observed. However, a further increase in the flow ratio to 2:10 resulted in a noticeable rise in the deposition rate. Since the argon flow rate was kept constant at 200 sccm across all samples prepared under varying nitrogen flows, the partial pressure of Ar remained largely unchanged. Therefore, variations in deposition rate attributable to the Ar atmosphere should be minimal. The observed increase in deposition rate at a higher N_2 flow rate of 40 sccm could be attributed to the formation of lighter or more volatile nitrogen-containing species (e.g., NO) during the reactive sputtering process, which may enhance the effective removal of material from the target or modify the plasma chemistry leading to a higher flux of deposition species.

Table 4. Effect of Nitrogen partial pressure on the Deposition Rate and Electrical Resistivity of ITO Thin Films

	Deposition rate nm/min	Sheet resistance Ω/□	Resistivity 10-4Ωcm
N0(A4)	39.9	23.5	11.26
N1	38.7	22.6	5.26
N2	47.8	21.0	6.02

Furthermore, SEM (Figure 5) and XRD (Figure 6) analyses consistently demonstrate that nitrogen doping significantly suppresses crystallinity and reduces surface roughness. The absence of sharp In_2O_3 diffraction peaks and the featureless surface morphology suggest that incorporated nitrogen atoms may disrupt the long-range order of the In_2O_3 lattice, potentially by occupying oxygen vacancy sites or forming amorphous indium oxynitride phases. This inhibition of crystalline growth results in a smoother but more electrically resistive film, as the increased disorder scatters charge carriers and reduces mobility. The combined structural evidence indicates

that nitrogen acts as a crystallinity-modifying agent, favoring the formation of an amorphous matrix over a polycrystalline one.

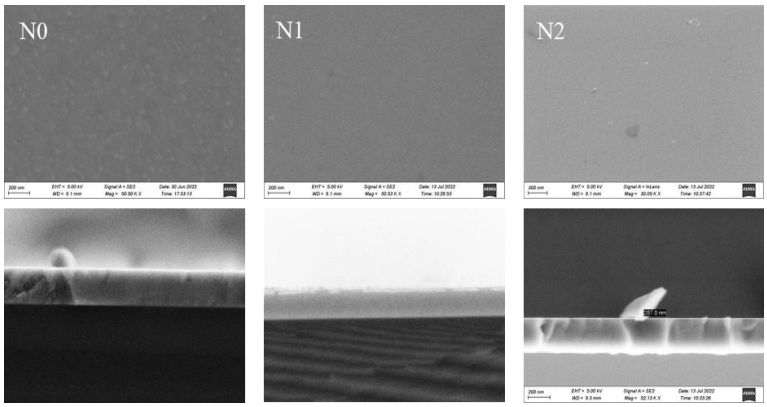

Figure 5. Surface and Cross-Sectional SEM Morphologies of ITO Thin Films Deposited with nitrogen

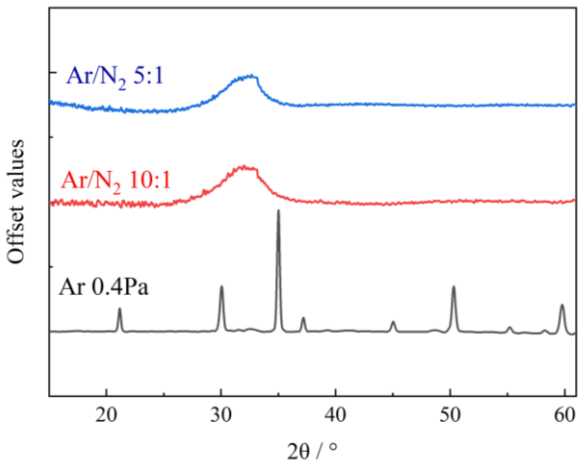

Figure 6. XRD Patterns of As-deposited ITO Thin Films sputtered with nitrogen

3.4. XPS Spectra Analysis of ITO thin films

The electrical performance of ITO thin films is strongly influenced by oxygen vacancy concentration and nitrogen doping. Systematic investigation of the content, chemical states, and bonding environments of oxygen and nitrogen therefore provides essential insights into the compositional and structural factors governing electrical behavior. Extensive theoretical and experimental studies have identified several possible chemical states for oxygen in ITO films, which can be categorized as follows [18]:

- **O1:** Lattice oxygen in stoichiometric In_2O_3.
- **O2:** Lattice oxygen associated with oxygen vacancies in non-stoichiometric In_2O_{3-x}.
- **O3:** Chemisorbed oxygen species (e.g., –OH, adsorbed O_2).

Figure 7 presents the O 1s XPS spectra of as-deposited ITO films prepared under

various sputtering conditions, revealing clear correlations between deposition parameters, oxygen chemical states, and electrical properties. The sample deposited at low Ar pressure (A4) exhibits a higher overall oxygen content with a dominant O1 peak (lattice oxygen in stoichiometric In_2O_3) and a weak O2 component (oxygen vacancy-related), indicating a near-stoichiometric composition that accounts for its higher resistivity due to limited carrier generation. As the Ar pressure increases, the intensity of the O2 peak rises progressively, reflecting an elevated oxygen vacancy concentration. This trend is attributed to more frequent collisions at higher pressure, which reduce the energy and flux of oxygen species reaching the substrate, thereby promoting non-stoichiometric In_2O_{3-x} formation and enhancing conductivity.

In contrast, increasing the sputtering power strengthens the O1 peak while suppressing the O2 contribution, suggesting a reduction in oxygen vacancies. The higher particle energy and improved oxidation conditions at elevated power favor a more complete oxide lattice, which supports better carrier mobility.

Introducing nitrogen into the sputtering atmosphere significantly alters the oxygen bonding environment: the O1 peak intensity decreases markedly, while the O2 and O3 (chemisorbed oxygen) contributions increase. Nitrogen incorporation competes with oxygen for lattice sites, disrupts the long-range order of In_2O_3, and stabilizes oxygen-deficient regions, consistent with the observed structural amorphization and modified electrical behavior.

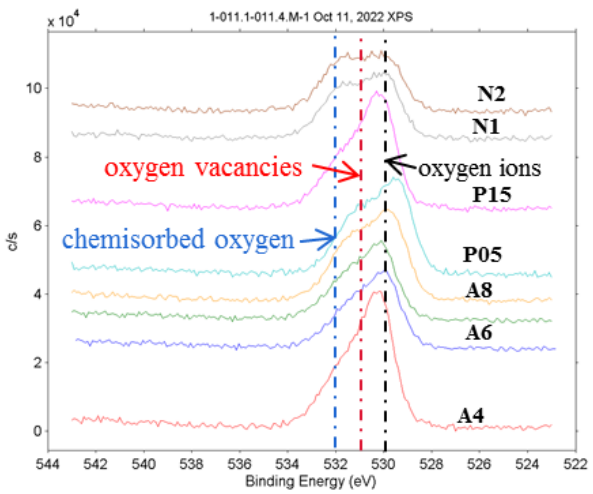

Figure 7. O 1s XPS spectra of as-deposited ITO films

Upon introduction of nitrogen into the sputtering atmosphere, distinct N 1s peaks appear around 396 eV in samples N1 and N2 **(Figure 8)**. The observed binding energy suggests the formation of In–N and/or Sn–N bonding, which is consistent with the measured changes in resistivity. These nitride-like phases likely modify the local electronic structure and carrier concentration, thereby influencing the overall electrical performance of the films.

The presence of nitrogen not only alters the chemical bonding network but also suppresses oxygen vacancy formation, leading to a more amorphous microstructure—as corroborated by XRD and SEM results. The combined XPS, electrical, and structural data highlight the critical role of anion engineering (O/N ratio and bonding configuration) in tuning the charge transport properties of sputtered ITO-based thin films. Further studies focusing on the precise coordination of nitrogen and its impact on defect equilibria would help clarify the underlying doping and compensation mechanisms.

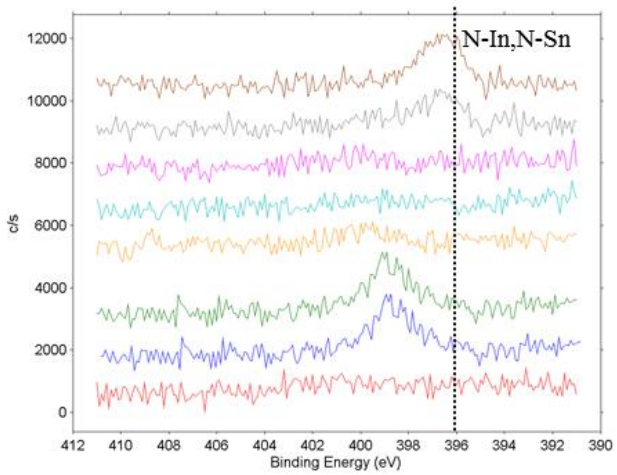

Figure 8. O1s XPS spectra of as-deposited ITO films

4. Discussion

4.1. Mechanism of Pressure-Dependent Control over Film Structure and Properties

The experimental results demonstrate that the working pressure during ITO film deposition directly influences plasma density, the kinetic energy of sputtered particles, and their transport path, thereby dictating the resultant microstructure and electrical properties. At a fixed power of 100 W, within a low-pressure environment (0.4 Pa), sputtered particles exhibit a long mean free path. They travel towards the substrate with high kinetic energy in a nearly ballistic trajectory, leading to enhanced surface diffusion capability upon arrival. This condition favors the formation of a dense, columnar grain structure. In this regime, the density of grain boundaries is relatively low, and carrier mobility is primarily limited by ionized impurity scattering.

As the pressure increases to 0.6 Pa, the plasma density rises, enhancing the probability of collisions between Ar^+ ions and the target, which results in a slight increase in sputtering yield. However, the kinetic energy of the particles is reduced due to more frequent collisions in the gas phase. The consequent attenuation of surface diffusion ability leads to more uniform grain sizes and a modest increase in

grain boundary density. Crucially, the reduced particle energy affects the relative arrival rates of different species. The deposition rate of oxygen atoms liberated from the target becomes lower than that of the metal atoms (In/Sn), preventing their sufficient recombination on the growing film surface. This imbalance explains the observed increase in oxygen vacancy concentration in the XPS spectra. As these oxygen vacancies act as donor defects, they significantly elevate the carrier concentration, leading to a reduction in resistivity to 5.73×10^{-4} Ω·cm.

When the pressure is further increased to 0.8 Pa, particle kinetic energy suffers greater loss, and surface diffusion is almost completely suppressed. The film becomes predominantly amorphous or nanocrystalline, as evidenced by the decreased XRD peak intensity, and the grain boundary density rises substantially. In this state, although grain boundary scattering intensifies, the continued increase in oxygen vacancy concentration provides a dominant positive contribution to carrier density. This effect outweighs the negative impact of enhanced scattering, causing resistivity to decrease further. The observed reduction in surface particles and agglomerations is likely linked to a more uniform deposition mode of low-energy particles, which inhibits abnormal grain growth and results in a finer, more homogeneous microstructure.

4.2. Mechanism of Power-Dependent Control over Film Structure and Properties

Increasing the sputtering power (from 50 to 150 W) directly modulates the energy of Ar^+ bombardment via a stronger sheath electric field, consequently affecting the sputtering yield, particle kinetic energy, and Sn doping efficiency.

At low power (50 W), the energy of Ar^+ ions is insufficient (＜300 eV), resulting in a low sputtering yield. The arriving particles lack the kinetic energy necessary to drive significant surface diffusion, leading to a predominantly amorphous film with a high density of defect states (e.g., dangling bonds, vacancy clusters). Carrier mobility is severely limited by strong localization scattering, resulting in high resistivity (12.3×10^{-4} Ω·cm).

When the power is increased to 100 W, the Ar^+ energy rises (to ~500 eV), significantly enhancing the sputtering yield and the kinetic energy of the deposited particles. This promotes surface diffusion and coalescence growth of grains, as evidenced by the increased grain size and stronger XRD diffraction peaks. Since the sputtering yield of Sn is higher than that of In, the Sn doping efficiency improves. This leads to a synergistic optimization of both carrier concentration and mobility, reducing the resistivity to 9.33×10^{-4} Ω·cm.

As the power is further increased to 150 W, the particle kinetic energy approaches saturation. However, localized target heating may cause an imbalance in the In/Sn ratio due to the preferential sputtering of In, potentially lowering the effective Sn doping efficiency. Concurrently, bombardment of the substrate by high-energy Ar^+

ions can introduce lattice damage (e.g., anti-site defects). Deep-level traps associated with such defects may partially compensate for the increased carrier concentration, causing the rate of resistivity reduction to slow down.

4.3. Mechanism of Reactive Atmosphere-Dependent Control over Film Structure and Properties

The introduction of nitrogen gas intricately modulates the chemical composition and electrical properties of ITO films through competitive adsorption, chemical doping, and phase transformation effects.

Under a low nitrogen partial pressure (10% N_2/Ar flow ratio), active nitrogen species (N^-, N_2^+) generated from plasma dissociation preferentially occupy oxygen vacancy sites, forming shallow donor levels. This significantly increases the carrier concentration, leading to a rapid decrease in film resistivity. Simultaneously, nitrogen doping suppresses the migration of oxygen vacancies, reducing defect accumulation at grain boundaries and resulting in lower surface roughness.

When the nitrogen partial pressure is increased to 20%, excessive nitrogen species react with In/Sn to form nitride phases (e.g., InN, Sn_3N_4). The crystal structure of these nitrides (e.g., hexagonal for InN) is incompatible with the cubic bixbyite structure of In_2O_3, promoting film amorphization, as indicated by reduced XRD peak intensity. The wide bandgap of these nitride phases impedes carrier transport. Furthermore, deep-level defects associated with bonds like N-In can act as carrier traps, causing the resistivity to increase again.

Additionally, at high nitrogen partial pressures, the dissociation of N_2 molecules consumes a portion of the plasma energy, initially having a negligible effect on the deposition rate. However, as a nitride layer forms on the target surface, its sputtering yield may differ from that of the oxide, potentially leading to the observed anomalous increase in deposition rate. The further reduction in surface roughness suggests that nitrogen doping inhibits island growth, favoring the formation of a uniform amorphous/nanocrystalline composite structure. Throughout this process, nitrogen-oxygen defect complexes may act as recombination centers, exacerbating carrier scattering and further degrading electrical performance.

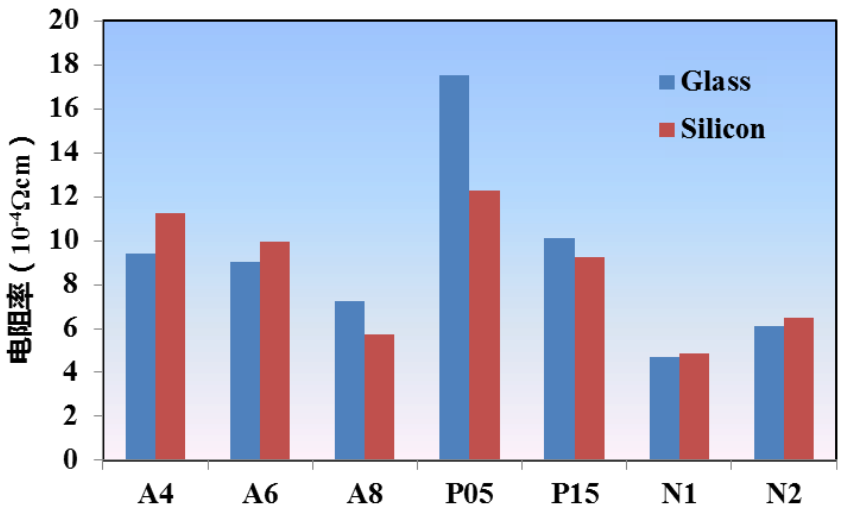

Figure 9. Resistivity of ITO thin films deposited on glass and Silicon substrate

5. Conclusions

For ITO thin films used for transparent conductive films and high temperature sensors, this study elucidates the effects of key magnetron sputtering parameters—working pressure, sputtering power, and nitrogen doping—on the deposition kinetics, microstructure, chemical state, and electrical properties of ITO thin films, establishing clear process-structure-property relationships. The results demonstrate that working pressure critically controls oxygen stoichiometry and conductivity. Low pressure (0.4 Pa) favors near-stoichiometric, well-crystallized films with higher resistivity. Increasing pressure enhances oxygen vacancy concentration, which acts as a dominant donor source, progressively reducing resistivity to 5.73×10^{-4} Ω·cm at the expense of crystallinity. Sputtering power primarily governs plasma energy and sputtering yield. Higher power (150 W) improves particle energy, surface diffusion, grain growth, and Sn doping efficiency, synergistically optimizing carrier concentration and mobility to lower resistivity. Excessive power may induce lattice damage and target composition imbalance. Nitrogen doping introduces complex chemical effects. At low flow, N atoms occupy oxygen vacancy sites as shallow donors, increasing carrier concentration and reducing resistivity. High N_2 partial pressure promotes the formation of incompatible nitride phases, causing amorphization and deep-level traps that increase resistivity. Nitrogen doping generally suppresses crystallization and surface roughening.

In summary, this work clarifies the individual and coupled effects of key deposition parameters and reveals their underlying mechanisms in tuning ITO film properties. The findings provide a solid theoretical and practical foundation for the precise fabrication of ITO films tailored for specific optoelectronic applications.

Acknowledgements

This research was supported by the National Key Laboratory Foundation of Science and Technology on Vacuum Technology and Physics Laboratory (HTKJ2023KL510003).

References

[1] Shigesato, Y., Yasui, I., & Paine, D. C. . (1995). ITO thin-film transparent conductors: microstructure and processing. JOM, 47(3), 47-50.

[2] Kim, D., Han, Y., Cho, J. S., & Koh, S. K. (2000). Low temperature deposition of ITO thin films by ion beam sputtering. Thin Solid Films, 377(2), 81-86.

[3] Hotovy, J., Huepkes, J., Boettler, W., Marins, E., Spiess, L., & Kups, T., et al. (2013). Sputtered ITO for application in thin-film silicon solar cells: relationship between structural and electrical properties. Applied Surface Science, 269(Mar.15), 81-87.

[4] Herrero, J., & C. Guillén. (2004). Improved ITO thin films for photovoltaic applications with a thin zno layer by sputtering. Thin Solid Films, 451, 630-633.

[5] Park, Y. S., Kim, E., Hong, B., & Lee, J. . (2013). Characteristics of ITO films with oxygen plasma treatment for thin film solar cell applications. Materials Research Bulletin, 48(12), 5115-5120.

[6] Khrypunova, A., Kudii, D., & Khrypunova, I. (2018). The optical and electrical properties ITO thin film. IEEE.

[7] Lee, S. M., Lee, Y. S., Shim, C. H., Choi, N. J., Joo, B. S., & Song, K. D., et al. (2003). Three electrodes gas sensor based on ITO thin film. Sensors & Actuators B Chemical, 93(1-3), 31-35.

[8] Giusti, G., Tian, L., Jones, I. P., Abell, J. S., & Bowen, J. . (2009). Microstructure-property relationships in thin film ITO. Thin Solid Films, 518(4), 1140-1144.

[9] Kim, S. M., Rim, Y. S., Keum, M. J., & Kim, K. H. . (2009). Study on the electrical and optical properties of ITO and azo thin film by oxygen gas flow rate. Journal of Electroceramics, 23(2-4), 341.

[10] Kim, S. I., Lee, K. W., Sahu, B. B., & Han, J. G. . (2015). Flexible oled fabrication with ITO thin film on polymer substrate. Japanese Journal of Applied Physics, 54(9), 090301.

[11] Wang, Y., Zhang, C., & Ding, G. . (2017). Fabrication and characterization of ITO thin film resistance temperature detector. Vacuum, 140, 121-125.

[12] Wen, L., Sahu, B. B., Yeom, G. Y., & Han, J. G. . (2021). Room temperature deposition of very thin and flexible crystalline ITO thin film using 3-d facing-magnetron sputtering plasma source. Vacuum, 193, 110520-.

[13] Zhao, X., Yang, K., Wang, Y., Chen, Y., & Jiang, H. . (2016). Stability and thermoelectric properties of ITOn:pt thin film thermocouples. Journal of Materials Science Materials in Electronics, 27(2), 1725-1729.

[14] X., H., Zhao, H., T., Li, S., W., & Jiang, et al. (2017). Effect of nitrogen doping on the thermoelectric properties of ITO-in2o3 thin film thermocouples. Thin Solid Films.

[15] ShenyongZhang, CongchunYang, ZhuoqingYao, JinyuanWang, HongDing, Guifu. (2019). Effect of nitrogen doping temperature on the resistance stability of ITO thin films. Journal of Alloys and Compounds: An Interdisciplinary Journal of Materials Science and Solid-state Chemistry and Physics, 778.

[16] Liu, Z., Liang, J., Li, J., Yang, M., & Xu, J. . (2021). Effect of nitrogen-doped concentration on the tcr of ITO thin films at high temperature. IEEE.

[17] Gulen, M., Yildirim, G., Bal, S., Varilci, A., Belenli, I., & Oz, M. . (2013). Role of annealing temperature on microstructural and electro-optical properties of ITO films produced by sputtering. Journal of Materials Science Materials in Electronics, 24(2), 467-474.

[18] Liu, Y., Jiang, H., Zhao, X., Liu, B., Jia, Z., & Liang, X., et al. (2023). Effects of nitrogen

doping and oxygen vacancies on thermoelectric properties of pt/n-doped ITO thin film thermocouples: first-principles calculations and experiments. Journal of Materials Science, 58(7), 3219-3230.